

# A Semantic-based Layer Freezing Approach to Efficient Fine-Tuning of Language Models

Jian Gu<sup>1</sup>, Aldeida Aleti<sup>1</sup>, Chunyang Chen<sup>2</sup>, Hongyu Zhang<sup>3</sup>

<sup>1</sup>Monash University, <sup>2</sup>Technical University of Munich, <sup>3</sup>Chongqing University

Correspondence: aldeida.aleti@monash.edu

## Abstract

Finetuning language models (LMs) is crucial for adapting the models to downstream data and tasks. However, full finetuning is usually costly. Existing work, such as parameter-efficient finetuning (PEFT), often focuses on *how to finetune* but neglects the issue of *where to finetune*. As a pioneering work on answering where to finetune (at the layer level), we conduct a semantic analysis of the LM inference process. We first propose a virtual transition of the latent representation and then trace its factual transition. Based on the deviation in transitions, we estimate the gain of finetuning each model layer, and further, narrow down the scope for finetuning. We perform extensive experiments across well-known LMs and datasets. The results show that our approach is effective and efficient, and outperforms the existing baselines. Our approach is orthogonal to existing efficient techniques, such as PEFT methods, offering practical values on LM finetuning.

## 1 Introduction

With the rapid advancements and notable performance of language models, their application has extended to numerous downstream tasks (Bommasani et al., 2021). Fine-tuning techniques are pivotal in augmenting the capabilities of language models (Raffel et al., 2019; Ouyang et al., 2022). For example, CODE LLAMA is a code-specialized LM and is finetuned on 100B tokens of Python code for a language-specialized variant (Touvron et al., 2023; Rozière et al., 2023). The Python variant provides better capabilities in code understanding and generation, since Python is most popular in programming (Carbonnelle, 2024; TIOBE, 2024).

Compared to their smaller pretrained predecessors, finetuning large LMs offers both advantages and disadvantages. On one hand, the vast number of model parameters triggers the emergent abilities of large LMs (Wei et al., 2022), leading to superior

performance across a variety of tasks, which serves as an excellent foundation for domain-specific finetuning. On the other hand, the extensive parameter size presents challenges for downstream finetuning. For instance, large LMs require greater memory costs and higher computational costs in finetuning.

The challenge is on the correlation between performance and efficiency of LM finetuning. There have been developed techniques such as model quantization and PEFT methods to improve efficiency (Rokh et al., 2022; Han et al., 2024). Model quantization reduces the precision of the model and data to reduce the burden of storage and computation. However, the performance of LM finetuning may be damaged to some extent. PEFT methods introduce additional parameters to learn the updates in LM finetuning, and then merge the updates into the LM. They reduce the memory costs but cannot save the computational cost. There has been relatively little work exploring the correlation between performance and efficiency, that is, whether the performance of LM finetuning can be improved while saving cost. To mitigate the gap, we propose utilizing the semantics in LM latent space to identify the layers that are more in need of finetuning, and freeze other layers to specify them being trainable.

Our intuition is that, by interpreting the LM’s functionality as a transition of semantics and comparing it with an idealized situation, we can estimate the deviation in each layer. The deviations can be used to evaluate the contribution of model layers, and further, as the evidence to decide which layers shall be trainable. Based on empirical experience and theoretical analysis, the deviations in semantic transitions greatly decide the effects of LM finetuning. By finding the model layer with the least deviation and shortening the process of backpropagation, the computation cost may be reduced and meanwhile, the finetuning effects can be improved. Efficient finetuning via layer-freezing is orthogonal with existing techniques, including model quantiza-

tion and PEFT methods, so can combine with them for the better computation-efficiency.

In this paper, we realize efficient finetuning by proposing an effective and reliable layer-freezing approach. That is, taking Semantic-based Efficient Fine-Tuning (SEFT) to balance the computational cost and the finetuning performance. First, on the shoulder of vocabulary-defined semantics (Gu et al., 2024), we study the phenomenon of semantic transition in LMs. By introducing an idealized transition process, we estimate the deviations in each model layer; Then, utilizing the deviations, our layer-freezing approach finds the layer whose deviation is the least and freezes the deeper layers; Last, to support a flexible cost-benefit tradeoff, we propose a deep-to-shallow policy for layer-freezing to fulfill the given budget. We also propose better budget plans for the cost-benefit tradeoff.

We evaluate our approach in fine-tuning diverse datasets on a wide range of modern LMs. Based on the results, our semantic-based layer-freezing approach performs better than the baselines. Combined with budget plans, our approach can further reduce the computation cost and improve the performance. We discuss the insights of efficient finetuning from the perspective of semantics and conclude the findings in finetuning LMs. The replication repository is attached as supplementary material.

Our contributions are as follows:

- We propose using the deviations in semantic transition to explain the process of LM inference, and further study the cost-benefit tradeoff in LM finetuning;
- We emphasize the importance of knowing where to finetune, through which we can improve the performance of LM finetuning and save the computation cost. We propose semantic-based layer-freezing as a solution;
- We conclude some findings on the behavior of LMs, which can contribute to future work in finetuning and analyzing LMs. Also, we propose planning the budget for a better cost-benefit tradeoff of LM finetuning.

## 2 Preliminaries

### 2.1 Semantic Field in LM Latent Space

Based on vocabulary-defined semantics, the semantics of latent representations can be regarded as the overlapping impact of “semantic fields” (Gu et al.,

2024). The semantic field is similar to the field term in physics, such as electric field, where the electric strength relies on the distance to the center of the field (the electric pole). The corresponding probabilities on the vocabulary of a representation can be directly computed with its locations in the semantic fields in the latent space, as shown in Figure 1. In contrast, in common practice, the representations in last-layer latent space will undergo a dimensional change to be computed as logits, and then be normalized as the probabilities on the vocabulary. The dimensional change causes entanglement of semantics, and exacerbates the computation complexity.

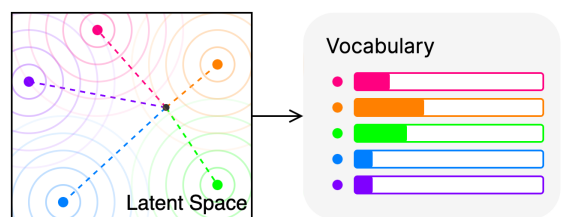


Figure 1: Vocabulary-defined semantics is demonstrated with a LM, whose vocabulary is a collection of colorful labels: (1) in the latent space (left), large color dots are the corresponding semantic bases of vocabulary labels. The small dark dot is the latent representation of a given data. The similarities of the data with semantic bases are regarded as logits; (2) on the vocabulary (right), the logits are normalized as probabilities, and the argmax label is *orange*. Consistently, the nearest semantic base to the latent representation is the *orange* one.

The semantics of LM latent space is decided by the semantic fields (Gu et al., 2024). For each label in the vocabulary, there is a corresponding semantic field in the latent space. The pole of a semantic field is called semantic base, representing an unmixed and purest meaning. If representations are closer to a semantic base, they tend to share the meaning of that semantic base. The semantic meaning of a representation in the latent space is decided by the overlapping impact of multiple semantic fields.

The computation of semantic bases is simple. At the LM input side, we multiply onehot embedding  $\vec{e}$  by the embedding matrix  $\mathbb{W}_i$  to obtain the semantic base  $\vec{r}_i = \vec{e} \cdot \mathbb{W}_i$ . At the LM output side, due to the opposite operation direction between the embeddings and the representations, we turn to use the pseudoinverse of the LM-head matrix  $\mathbb{W}_o^+$ . We multiply onehot embedding  $\vec{e}$  by the pseudoinverse matrix to obtain the semantic base  $\vec{r}_o = \vec{e} \cdot \mathbb{W}_o^+$ . Since LM vocabulary is required in the computations, semantic bases only exist in the embedding latent space and the last-layer latent space.

## 2.2 Semantic-based Loss Computation

Based on the local isotropy of LM latent space (Cai et al., 2021), the logits in LM training and inference can be computed via similarity measurement (with semantic base), instead of matrix multiplication (with LM-head matrix). The logits computed in this way is termed as "similarity-based logits" (Gu et al., 2024). It proves to have the same effects as the common practice of logits computation, and shows advantages in disentangling the semantics.

In LM finetuning, the logits will be used in loss computation. Taking the cross-entropy loss as an example, we compute the similarities between the given latent representation with semantic bases as similarity-based logits, and then compute with the ground truth for the loss, as shown in Algorithm 1.

---

### Algorithm 1 Semantic Cross-Entropy Loss

---

**Require:**  $N$  semantic bases  $\vec{b}_i$ ; ground truth label  $l$ ; last-layer latent repr  $\vec{r}$   
**Ensure:** optimization target  $loss$   
logits  $\leftarrow$  init\_1d\_tensor( $N$ )  
**for**  $i \leftarrow 0$  **to**  $N$  **do**  
  logits[ $i$ ]  $\leftarrow$  cosine\_similarity( $\vec{r}$ ,  $\vec{b}_i$ )  
**end for**  
loss  $\leftarrow$  cross\_entropy\_loss(logits,  $l$ )

---

Further, leveraging the disentanglement effects of similarity-based logits, we can compute the loss merely with the corresponding ground truth. In the loss computation, the latent representation is only computed with one semantic base solely, instead of with all semantic bases, as shown in Algorithm 2. In terms of effect, it optimizes the latent representation to make it steer towards the corresponding semantic base. The cosine-similarity loss is better in computation cost, and its computation shows an intuitive geometric meaning in the latent space.

---

### Algorithm 2 Semantic Cosine-Similarity Loss

---

**Require:**  $l$ -th semantic base  $\vec{b}_l$  (for ground truth label  $l$ ); last-layer latent repr  $\vec{r}$   
**Ensure:** optimization target  $loss$   
loss  $\leftarrow$  1 - cosine\_similarity( $\vec{r}$ ,  $\vec{b}_l$ )

---

## 3 Semantic-based Efficient Fine-Tuning

### 3.1 Transitions on Semantics

In next-token prediction, the last token in the given input is used as the medium to compute the next

token, denoted as *medium token*. Influenced by the embeddings of other tokens and the parameters in model layers, the medium token will undergo a transition on its semantic meaning, denoted as *semantic transition*. LM finetuning has effects on semantic transition, and the differences before and after finetuning are illustrated in Figure 2. We define the involved concepts as below.

*Transition Trace.* For a given sequence of  $n$  tokens,  $t_1, t_2, \dots, t_n$ , assume a  $m$ -layer LM will predict the next token  $t_{n+1}$ , the representation of  $t_n$  undergoes a semantic transition from semantic meaning  $i$  to  $j$ . The *factual* representation in each layer is denoted as  $f_0, f_1, f_2, \dots, f_m$  ( $f_0$  is the onehot embedding, equals to  $i$ ; while  $f_m$  is the last-layer representation, equals to  $j$ ), so the semantic transition defined by these representations is a *transition trace*.

*Transition Route.* For a given sequence of  $n$  tokens,  $t_1, t_2, \dots, t_n$ , assume a  $m$ -layer LM will predict the next token  $t_{n+1}$ , the representation of  $t_n$  undergoes a semantic transition. The semantic meaning of the token is  $i$  and that of the ground truth is  $k$ . An idealized semantic transition from  $i$  to  $k$  is defined as a *transition route*. The *virtual* representation in each layer is denoted as  $v_0, v_1, v_2, \dots, v_m$  ( $v_0$  is the onehot embedding, equals to  $i$ ; while  $v_m$  is the representation of the ground truth, equals to  $k$ ).

Following the principle of Occam’s razor, that is, taking the simplest explanation for an observation is most likely to be correct, we take a hypothesis that, *For a given LM, the changes to the representations between neighboring layers shall be simple*. Therefore, the idealized transition route is straight from the initial embedding (a semantic base in the embedding latent space) of the medium token to the representation of the ground truth (a semantic base in the last-layer latent space).

For a straight transition route, the virtual representations shall be the interpolated results. The virtual latent representation in the transition route is termed as *semantic anchor*. The semantic anchor in each model layer can be estimated using the semantic bases of two sides and linear interpolation. For a given token, we note the semantic anchor at layer  $k$  of a  $m$ -layer LM as  $\vec{r}_k$  (the computation formula is  $\vec{r}_k = (1 - \frac{k}{m}) \vec{r}_i + \frac{k}{m} \vec{r}_o$ ).

*Transition Deviation.* For a semantic transition of a  $m$ -layer LM, the *factual* representation in each layer of the transition trace is  $f_0, f_1, f_2, \dots, f_m$ , and the *virtual* representation in each layer of the transition route is  $v_0, v_1, v_2, \dots, v_m$ . The deviation of the

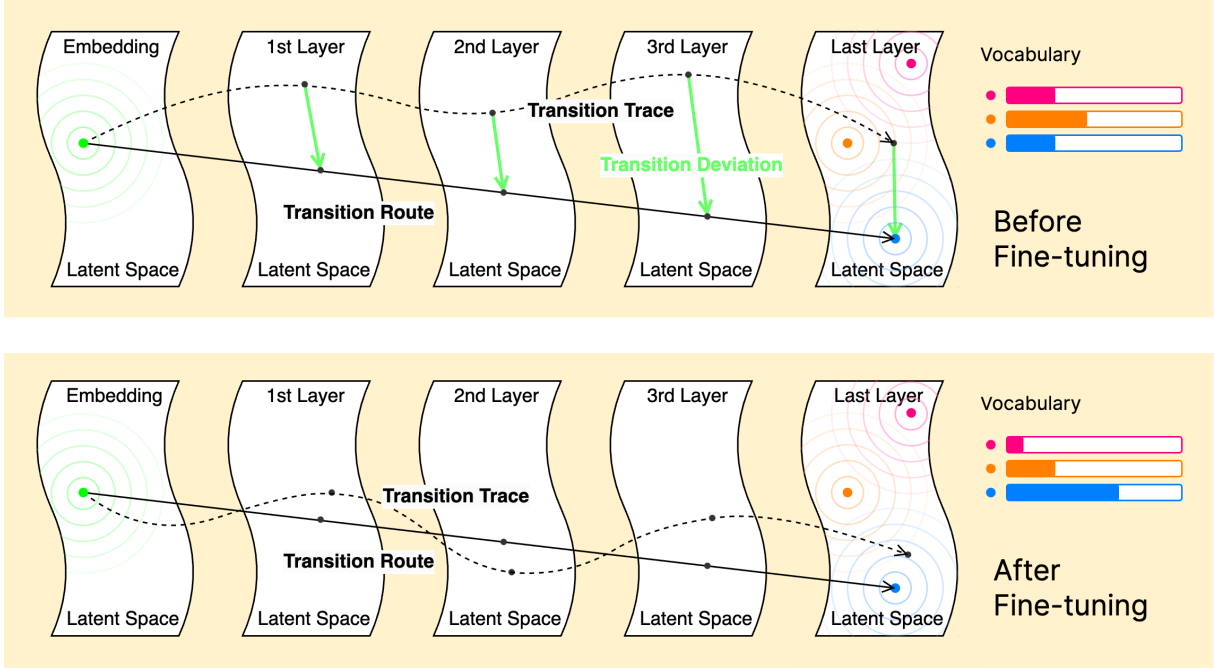


Figure 2: The transition of semantics is illustrated with a 4-layer LM, whose vocabulary is a collection of colorful labels. The green dot is the medium token (input-side semantic base) and the blue dot is the ground truth (output-side semantic base). The dashed curve (transition trace) represents the factual semantic transition of the medium token, defined by the dark dots (factual latent representations) in each latent space. The solid curve (transition route) represents the virtual semantic transition of the medium token, defined by the medium token and the ground truth via interpolation. The interpolated results in each latent space are semantic anchors (virtual latent representations), marked as dark dots. The green lines (transition deviation) indicate the differences between the factual and virtual latent representations, and they differ before and after LM finetuning: (1) before finetuning (upper), the semantic deviation in each layer is obvious. The latent representation in last-layer is semantically far from the ground truth, so the argmax label is *orange*; (2) after finetuning (below), the semantic deviation in each layer is reduced. The latent representation in last-layer is semantically close to the ground truth, so the argmax label is *blue*.

factual representation to the virtual representation in each layer can be measured (such as using cosine similarity), denoted as  $d_0, d_1, d_2, \dots, d_m$  ( $d_0 = 0$  always stands since  $f_0 = v_0$ ), The deviations in the semantic transition are called *transition deviations*.

The transition deviations before and after finetuning differ. Theoretically and empirically, LM finetuning tends to reduce the deviations. For a given medium token, in LM finetuning, the transition trace will approach the corresponding transition route. The approach will be reflected in the deviation in each layer. By probing the situation of each layer, the transition deviation will be reduced as well. That means, the latent representation will approach the corresponding semantic anchor.

Further, transition deviations can be regarded as the evaluation metrics of the capability of model layers. In the latent space of the LM last-layer, the representation of the medium token is intended to be close enough to the semantic base (namely the ground truth). If the latent representations in

the middle layers are close to the corresponding semantic anchor, then the latent representations in the last layer are likely to be close to the semantic base. Therefore, leveraging the transition deviations, model layers can be finetuned selectively.

### 3.2 Semantic-based Layer-Freezing

In next-token prediction, via LM finetuning, the last-layer latent representation of the medium token is close enough to the ground truth. The finetuning process can be explained as divide-and-conquer: If the factual representation is closer to the virtual one in the  $k$ -th layer, then they tend to be closer as well in the  $(k + 1)$ -th layer. By making the latent representation close enough to the semantic anchor in each layer, the representation in the last-layer tends to be close to the ground truth.

Based on the explanation, we propose a layer-freezing method to accelerate finetuning. The idea is simple: *instead of finetuning from the first-layer, we find the layer where the deviation is the least*

and then finetune from there to the last-layer. We call the layer having the least deviation as end-of-freezing layer, short as *eof-layer*. The deeper layers will be frozen so only the eof-layer and shallower layers are trainable, as shown in Algorithm 3.

---

### Algorithm 3 SEFT Layer-Freezing

---

**Require:** latent\_reprs, semantic\_anchors

**Ensure:** eof\_layer\_id

```

deviations  $\leftarrow$  empty list
for layer_id  $\leftarrow$  0 to layer_num do
    deviation  $\leftarrow$  1 - cosine_similarity(
        latent_reprs[layer_id],
        semantic_anchors[layer_id])
    deviations.append(deviation)
end for
eof_layer_id  $\leftarrow$  argmin(deviations)

```

---

For a given dataset, the computation cost of back-propagation is decided by the depth of eof-layers, we can count the depths to know the cost-saving of layer-freezing. To the opposite, we can have a budget plan and force the depths of eof-layers to fulfill the budget. In this way, we can control the cost-saving by planning the depth of eof-layers.

### 3.3 Budget for Layer-Finetuning

To balance the effectiveness and cost of model finetuning, we incorporate a budget to determine the extent of layer-freezing based on specific requirements (see Appendix A). This budget represents the number of model layers to fine-tune for a given dataset. It controls the efficiency of LM finetuning, for example, we tend to give a low budget for LM finetuning if we want a high efficiency.

*Budget Plan.* Similar to the common practice of finetuning half layers, we design budget plans to control the cost-benefit tradeoff. For a given model of  $m$  layers, we make the amount of data, that is assigned to finetuning layers between the eof\_layer to the last layer, following the relative proportion of the growth sequence: (1) Following geometric growth, we take the growth ratio as 2. Then, the amount of data assigned for finetuning follows the relative proportion of 1, 2, 4, ...,  $2^{m-1}$ ; (2) Following arithmetic growth, we make the initial term the common difference between terms. Then, the amount of data assigned for finetuning follows the relative proportion of 1, 2, 3, ...,  $m - 1$ .

*Budget Infilling.* For a given dataset, if the budget cannot be infilled completely with the data, the

		CARER	MRPC	SST5	TREC	WebSS
Class Num.		6	2	5	6	8
Data Num.	Train	16,000	4,076	8,544	5,452	10,060
	Test	2,000	1,725	2,210	500	2,280
Avg. Prompt Length		25.6	61.0	28.0	17.1	27.8

Table 1: Stats of text understanding datasets.

infilling order will affect the cost-benefit tradeoff. We introduce two practices for budget infilling: (1) Breadth-First (BF) fills eof-layers in the deep layers, and then shallower layers; (2) Depth-First (DF) fills eof-layers in all layers evenly, until layers are infilled successively from deep to shallow. We illustrated with a model having four layers, following geometric growth, as shown in Figure 3.

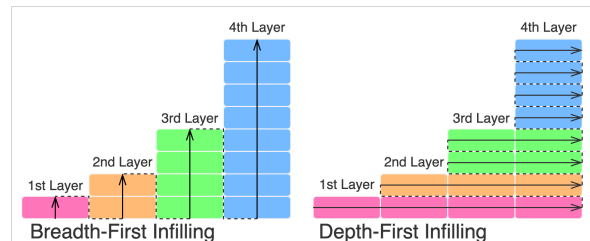


Figure 3: The order of budget infilling for a 4-layer model is: first red, then orange, then green, and finally blue shares. In breadth-first infilling, the color of shares is decided by layer. First let eof-layers be in first-layer until the layer is full (red); then let them be in second-layer until full (orange); then be in third-layer (green); and finally be in last-layer (blue). In depth-first infilling, the color of shares is decided by the position in layers. First let eof-layers be in first-share of all layers, from deep to shallow layers; then let them be in second-share of all layers; and then repeat the practice in the third share, fourth share, until the budget of each layer is satisfied in the proper order (red, orange, green, and blue).

## 4 Experiments and Results

### 4.1 Setup

*Datasets.* We use 5 established datasets, covering common text understanding tasks: emotion recognition: CARER (Saravia et al., 2018); similarity detection: MRPC (Dolan and Brockett, 2005); sentiment analysis: SST5 (Socher et al., 2013); and general text classification: TREC (Voorhees and Tice, 2000) and WebSS (Phan et al., 2008). The statistics of datasets are shown in Table 1.

*Models.* we conduct experiments with a wide range of Pythia scales (160M-2.8B) (Biderman et al., 2023). Besides, we also use the state-of-the-art open-source LLM in the experiments: Llama-3

	Pythia					Llama3
	Small	Medium	Large	XL	XXL	8B
Model Size	160M	410M	1.0B	1.4B	2.8B	8.0B
Head Num.	12	16	8	16	32	32
Layer Num.	12	24	16	24	32	32
Dimension	768	1,024	2,048	2,048	2,560	4,096
Vocabulary	50,304					128,256

Table 2: Stats of Pythia and Llama3 models.

(8.0B)<sup>1</sup>. The details are available in Table 2.

*Baselines.* LIFT is the state-of-the-art in layer-wise LM finetuning on saving the computation cost. It takes a front-to-end selection policy to prioritize the layer to finetune (Zhu et al., 2024). However, it only finetunes one layer each time, which may damage its performance. We relax its restrictions for a stronger baseline by letting more layers be trainable while the computation cost is the same. In addition, we also compare our approach SEFT with two intuitive finetuning practices: full-layer finetuning and half-layer finetuning (denoted as Naive[full] and Naive[half]). The former is to finetune all model layers, while the latter is to finetune only the last half model layers.

*Metrics.* For effectiveness, we use *accuracy* to measure whether the predicted next-token is the ground truth. For efficiency, we use the “cost-saving” ratio as a new metric, representing the saved computation cost in backpropagation. A large ratio is better.

*Pipeline.* We conduct LM finetuning experiments to compare our approach with other layer-freezing practices. Since LIFT is designed to save around 50% computation cost in backpropagation, we restrict our approach to the same computation cost for a fair comparison (on effectiveness). The details on the implementation are in Appendix A.

## 4.2 Performance Evaluation

We evaluate the performance of our approach and the baselines in LM finetuning: finetune the LMs on the training set, and do predictions on the test set. We compute the accuracy by comparing the predicted tokens with the ground truth.

As shown in Table 3, based on the average accuracy score, on 5 out of 6 models, SEFT performs better than others, while on the other model, its performance is very close to the best. Compared with common practices Naive[full] and Naive[half], LIFT shows superiority in the performance while

LLM	Method	Dataset					Avg.
		CARER	MRPC	SST5	TREC	WebSS	
Pythia-S	Naive[full]	0.591	0.665	0.286	0.904	0.822	0.654
	Naive[half]	0.596	0.665	0.311	0.872	0.796	0.648
	LIFT[half]	0.691	0.665	0.405	0.882	0.811	0.691
	SEFT[half]	0.802	0.665	0.409	0.872	0.809	0.711
Pythia-M	Naive[full]	0.348	0.665	0.286	0.832	0.788	0.584
	Naive[half]	0.757	0.685	0.438	0.904	0.815	0.720
	LIFT[half]	0.546	0.665	0.447	0.898	0.829	0.677
	SEFT[half]	0.821	0.665	0.451	0.938	0.802	0.735
Pythia-L	Naive[full]	0.895	0.665	0.248	0.896	0.852	0.711
	Naive[half]	0.802	0.725	0.286	0.916	0.870	0.720
	LIFT[half]	0.887	0.667	0.526	0.954	0.869	0.781
	SEFT[half]	0.908	0.726	0.524	0.954	0.853	0.793
Pythia-XL	Naive[full]	0.867	0.665	0.466	0.906	0.849	0.750
	Naive[half]	0.785	0.665	0.310	0.934	0.874	0.713
	LIFT[half]	0.899	0.690	0.557	0.950	0.904	0.800
	SEFT[half]	0.908	0.665	0.546	0.958	0.899	0.795
Pythia-XXL	Naive[full]	0.880	0.665	0.535	0.932	0.869	0.776
	Naive[half]	0.838	0.665	0.548	0.932	0.897	0.776
	LIFT[half]	0.348	0.665	0.552	0.954	0.904	0.684
	SEFT[half]	0.907	0.700	0.556	0.964	0.903	0.806
Llama3-8B	Naive[full]	0.348	0.665	0.287	0.402	0.736	0.487
	Naive[half]	0.885	0.781	0.530	0.932	0.877	0.805
	LIFT[half]	0.827	0.771	0.590	0.948	0.898	0.807
	SEFT[half]	0.923	0.737	0.579	0.964	0.904	0.821

Table 3: Accuracy of layer-freezing methods (on the diverse datasets and models).

our approach SEFT shows stable and obvious improvements. Besides, the advantages of SEFT vary on the datasets. On WebSS, SEFT performs the best only in the case where the model is Llama3, but the performance gap to the best is not obvious. However, on MRPC, SEFT cannot show stable improvements, especially when the model is Llama3. The reason is that, the class number of the MRPC dataset is only 2, that means, the situation of semantic transition is very simple, thereby the deviations in the process may not be very helpful.

It is noteworthy that Naive[full] perform worse than others, and even worse than Naive[half]. It is counter-intuitive since full-layer finetuning is updating all layers and requires a larger computation cost than Naive[half]. However, in our understanding, it may caused by the difference in the effects of deep and shallow model layers. Usually, deep layers learn the macro features while shallow layers learn the micro features (So et al., 2019; Brown et al., 2020). It means, *when the learning rate is fixed in LM finetuning, the update in deep layers shall be less frequent than that in shallow layers.* It also explains the reason why both Naive[full] and Naive[half] perform not as well as LIFT or SEFT: Naive[full] updates deep layers too often while Naive[half] updates deep layers too seldom.

In addition, we studied the effects of finetuning different LM modules, and further analyzed the advantages of our approach in LM finetuning with the illustrations on transition deviations in Appendix B.

<sup>1</sup><https://github.com/meta-llama/llama3>

Variant	Dataset					Avg.
	CARER	MRPC	SST5	TREC	WebSS	
LIFT[half]	0.827	0.771	0.590	0.948	0.898	0.807
LIFT[half][reverse]	0.891	0.665	0.559	0.754	0.882	0.750
LIFT[half][vanilla]	0.760	0.668	0.577	0.928	0.795	0.745
SEFT[half]	0.923	0.737	0.579	0.964	0.904	0.821
SEFT[half][base]	0.889	0.665	0.231	0.942	0.132	0.572
SEFT[half][ce-loss]	0.899	0.665	0.570	0.954	0.896	0.797

Table 4: Accuracy of layer-freezing variants (on the diverse datasets, using Llama3-8B).

### 4.3 Ablation Study

We study the variants of layer-freezing methods LIFT and SEFT, to know how different designs in their practice affect the performance.

For LIFT, we check the case where more layers are gradually trainable. Since deeper layers are frozen, it corresponds to the case where we finetune data whose eof-layers lie in shallower layers, and gradually we finetune data whose eof-layers lie in deeper layers. It is a reversed case of the baseline implementation, denoted as LIFT[half][reverse]. Besides, we also check the performance of the vanilla implementation, denoted as LIFT[half][vanilla].

As shown in Table 4, when the finetuning order of data is reversed, LIFT[half][reverse] cannot perform as well as LIFT[half]. Due to the computation direction being from deep layers to shallow layers, it is intuitively recognized that, the changes in deep layers may cause effects of shallow layers. Based on the results of the LIFT[half][reverse] variant, the effects is confirmed to be more likely negative. In the perspective of semantic transition, *the finetuning effort on shallower layers may be damaged by the finetuning effort in deeper layers.*

Similarly, the results of LIFT[half][vanilla] are not as good as the LIFT[half]. Their difference is that, the former only makes the eof-layer trainable, while the latter finetune all layers between eof-layer to last-layer. It indicates that, merely finetuning deep layers cannot guarantee smaller deviations in the shallow layers, or the deviations require further processing. In other words, *a reduction of the deviation in deep layers cannot promise a sufficient reduction on the deviation in shallow layers.* In addition, the comparison further indicates that, our approach SEFT is better than the baseline LIFT, since it already performs better than the enhanced version of LIFT.

For SEFT, we check the case where the semantic base (at the output side) takes the role of semantic anchor, denoted as SEFT[half][base]. It indicates

the common practice to detect how the model capability improves across different layers. That is, probing the latent representations at the middle model layer, and using them for logits computation as an estimation for LM interpretability. In addition, we check the case where letting the cross-entropy loss be the deviation measurement, denoted as SEFT[half][ce-loss], since cross-entropy is commonly used in logits computation. In contrast, the cosine-similarity loss is novel and only focuses on the corresponding ground truth.

As shown in Table 4, compared with our approach SEFT[half], the variants perform worse. SEFT[half][base] is using semantic base at the output side to measure the deviation, not semantic anchor. Even though the computation is similar, the practice lacks intuitive explanations. The reason why semantic anchor is useful is because it can approximate the transition on semantics. In contrast, semantic base cannot reveal the process so it fails to well perform. In common probing techniques, the latent representations in middle layers are taken to compute logits, which is equivalent to computing the similarities between latent representations with the semantic base (Gu et al., 2024). We conclude that, *the capability of semantic anchor in modeling semantic transitions shows better interpretability and guarantees better effects in LM probing.*

Meanwhile, SEFT[half][ce-loss] is a common practice in model finetuning, that is, taking cross-entropy loss, not cosine-similarity loss. Since cross-entropy loss is do computation with all ground truths, not merely with the corresponding one, as did by cosine-similarity loss, the former one involves more constraints than the latter one. It indicates that SEFT[half][ce-loss] will be slower in convergence, and further explains why this variant cannot perform as well as SEFT[half] when training for the same epoch. Based on our analysis, they tend to have similar performance when doing model finetuning for an unlimited number of epochs until convergence. In our understanding, *a less constrained loss function indicates a more straightforward convergence process, and therefore tends to perform better in LM finetuning.*

## 5 Analysis on Cost-Benefit Tradeoff

We study the performance and cost-benefit trade-off of budget plans and infilling practices to layer-freezing. For example, a geometric-growth budget with breadth-first infilling is denoted as geom[bf].

As shown in Table 5, the budget for cost-benefit tradeoff is useful to both LIFT and our approach SEFT, while our approach still have better performance in most settings. In comparisons, the arithmetic-growth budget shows similar performance to the geometric-growth budget. Meanwhile, the practice of depth-first infilling tends to perform better and more stably than breadth-first infilling.

Budget	Dataset					Avg.
	CARER	MRPC	SST5	TREC	WebSS	
LIFT[half]	0.827	0.771	0.590	0.948	0.898	0.807
LIFT[geom][bf]	0.898	0.719	0.517	0.952	0.876	0.792
LIFT[geom][df]	0.895	0.775	0.581	0.958	0.887	0.819
LIFT[arith][bf]	0.887	0.772	0.572	0.960	0.889	0.816
LIFT[arith][df]	0.897	0.773	0.589	0.950	0.887	0.819
SEFT[half]	0.923	0.737	0.579	0.964	0.904	0.821
SEFT[geom][bf]	0.906	0.665	0.586	0.962	0.855	0.795
SEFT[geom][df]	0.920	0.711	0.607	0.970	0.921	0.826
SEFT[arith][bf]	0.921	0.752	0.391	0.964	0.911	0.788
SEFT[arith][df]	0.914	0.751	0.588	0.964	0.914	0.826

Table 5: Accuracy of layer-freezing methods with different budget plans and infilling practices (on the diverse datasets, using Llama3-8B).

As shown in Table 6, compared with geometric-growth, the budget of arithmetic-growth saves more computation costs. The reason is that, for a model of the same number of layers, the arithmetic-growth increases slower than the geometric-growth, so the budget of the latter is not likely to be fulfilled. For geometric-growth, eof-layers can fill in deep layers but cannot fill in shallow layers. Also, depth-first infilling can save more than the breadth-first infilling. The reason is similar, more eof-layers tend to be in shallow layers than in deep layers.

Budget	Dataset					Avg.
	CARER	MRPC	SST5	TREC	WebSS	
Naive[full]	0.000	0.000	0.000	0.000	0.000	0.000
Naive[half]	0.500	0.500	0.500	0.500	0.500	0.500
LIFT[half]	0.484	0.483	0.484	0.484	0.484	0.484
SEFT[half]	0.484	0.483	0.484	0.484	0.484	0.484
[geom][bf]	0.374	0.312	0.346	0.328	0.355	0.343
[geom][df]	0.616	0.583	0.601	0.589	0.604	0.598
[arith][bf]	0.614	0.613	0.613	0.609	0.615	0.613
[arith][df]	0.644	0.640	0.644	0.642	0.645	0.643

Table 6: Backpropagation cost-saving of layer-freezing methods with different budget plans (on the diverse datasets, using Llama3-8B).

Considering the efficiency and cost-benefit tradeoff, the budget of arithmetic-growth shows equivalent performance but saves more computation costs. Also, the practice of depth-first infilling is better than breadth-first infilling. Based on the results, an arithmetic-growth with depth-first infilling

saves around 1/3 more computation cost and has a slightly better performance. The reason explaining why the combination is performant is the same as discussed, *when the learning rate is fixed in LM finetuning, the update in deep layers shall be less frequent than that in shallow layers.*

## 6 Related Work

Leveraging the layered structure of neural models, the concept of layer-freezing was proposed decades ago, but mainly for deep belief networks (DBN) (Hinton, 2009). DBN is a stack of directed sigmoid belief network (SBN) (Neal, 1992) and an indirected restricted boltzmann machine (Hinton, 2017). The backpropagation is only applied to finetune the restricted boltzmann machine, while the dependencies between other layers are not bidirectional. Therefore, progressively training each layer is proposed as a greedy strategy for training DBN (Hinton et al., 2006; Bengio et al., 2006).

In the era of language models, there has been little significant work studying layer-freezing for efficient finetuning, while the focus often lies on parameter-efficient, namely reducing the amount of trainable parameters, instead of computation-efficient (Pan et al., 2024; Zhu et al., 2024). One reason is the complexity and interpretability of language models. Besides, the correlation between model layers is not intuitive, and the effects of bidirectional dependencies on layer-wise finetuning have not been studied. Another reason is that, the prior work on PEFT shows similar effects on reducing the number of trainable parameters, or even making the trainable parameters detachable.

## 7 Conclusion

In this paper, we have proposed the concept of semantic transition. By defining semantic trace and semantic route as factual and virtual transitions, we explain LM finetuning as the process of letting the factual one steer to the virtual one in latent space. Further, we propose semantic-based layer-freezing to accelerate LM finetuning, by finding the layer with the least deviation and freeze the deeper layers. Based on our results, semantic-based layer-freezing provides better performance than the state-of-the-art as well as the common practices. Moreover, our work explores the effects of budget plans on the cost-benefit tradeoff for layer-freezing. In return, the effectiveness of our lay-finetuning approach validates the usefulness of semantic transition.



## Limitations

In this paper, we proposed semantic transition as a new perspective on the LMs’ functionality, and also, suggested using the deviations in semantic transition to reduce the computation cost in LM finetuning, while maintaining and even improving the performance of LM finetuning.

In our understanding, our approach is leveraging the intuition to estimate the semantic trace. In our practice, we are following the principle of Occam’s razor. However, there is no evidence showing it leads to the optimal choice. Besides, choosing the layer with the least deviation as the layer-freezing layer is an empirical practice. In a high-dimensional latent space, the representations tends to be orthogonal to others (including the semantic anchors) (Vershynin, 2018), so the changes in deviations is not that intuitive. There may be potential evidence to support other better choices.

The semantic transition is based to the similarity measurement between latent representations and semantic bases (at both sides of LMs) or semantic anchors (in middle layers). The theoretical support is the local isotropy of LM latent space (Cai et al., 2021), hence our approach is limited in LMs whose latent space fulfills isotropy or local isotropy.

## Acknowledgments

We sincerely thank DUG Technology for providing the computing resources. Their support greatly facilitated our research efforts.

## References

- Yoshua Bengio, Pascal Lamblin, Dan Popovici, and H. Larochelle. 2006. [Greedy layer-wise training of deep networks](#). In *Neural Information Processing Systems*.
- Stella Biderman, Hailey Schoelkopf, Quentin G. Anthony, Herbie Bradley, Kyle O’Brien, Eric Hallahan, Mohammad Aflah Khan, Shivanshu Purohit, USVSN Sai Prashanth, Edward Raff, Aviya Skowron, Lintang Sutawika, and Oskar van der Wal. 2023. [Pythia: A suite for analyzing large language models across training and scaling](#). *ArXiv*, abs/2304.01373.
- Rishi Bommasani, Drew A. Hudson, Ehsan Adeli, Russ Altman, Simran Arora, Sydney von Arx, Michael S. Bernstein, Jeannette Bohg, Antoine Bosselut, Emma Brunskill, Erik Brynjolfsson, S. Buch, Dallas Card, Rodrigo Castellon, Niladri S. Chatterji, Annie S. Chen, Kathleen A. Creel, Jared Davis, Dora Demszky, Chris Donahue, Moussa Doumbouya, Esin Durmus, Stefano Ermon, John Etchemendy, Kawin Ethayarajh, Li Fei-Fei, Chelsea Finn, Trevor Gale, Lauren Gillespie, Karan Goel, Noah D. Goodman, Shelby Grossman, Neel Guha, Tatsunori Hashimoto, Peter Henderson, John Hewitt, Daniel E. Ho, Jenny Hong, Kyle Hsu, Jing Huang, Thomas F. Icard, Saahil Jain, Dan Jurafsky, Pratyusha Kalluri, Siddharth Karamcheti, Geoff Keeling, Fereshte Khani, O. Khattab, Pang Wei Koh, Mark S. Krass, Ranjay Krishna, Rohith Kuditipudi, Ananya Kumar, Faisal Ladhak, Mina Lee, Tony Lee, Jure Leskovec, Isabelle Levent, Xiang Lisa Li, Xuechen Li, Tengyu Ma, Ali Malik, Christopher D. Manning, Suvir Mirchandani, Eric Mitchell, Zanele Munyikwa, Suraj Nair, Avani Narayan, Deepak Narayanan, Benjamin Newman, Allen Nie, Juan Carlos Niebles, Hamed Nilforoshan, J. F. Nyarko, Giray Ogut, Laurel J. Orr, Isabel Papadimitriou, Joon Sung Park, Chris Piech, Eva Portelance, Christopher Potts, Aditi Raghunathan, Robert Reich, Hongyu Ren, Frieda Rong, Yusuf H. Roohani, Camilo Ruiz, Jack Ryan, Christopher R’e, Dorsa Sadigh, Shiori Sagawa, Keshav Santhanam, Andy Shih, Krishna Parasuram Srinivasan, Alex Tamkin, Rohan Taori, Armin W. Thomas, Florian Tramèr, Rose E. Wang, William Wang, Bohan Wu, Jiajun Wu, Yuhuai Wu, Sang Michael Xie, Michihiro Yasunaga, Jiaxuan You, Matei A. Zaharia, Michael Zhang, Tianyi Zhang, Xikun Zhang, Yuhui Zhang, Lucia Zheng, Kaitlyn Zhou, and Percy Liang. 2021. [On the opportunities and risks of foundation models](#). *ArXiv*, abs/2108.07258.
- Tom B. Brown, Benjamin Mann, Nick Ryder, Melanie Subbiah, Jared Kaplan, Prafulla Dhariwal, Arvind Neelakantan, Pranav Shyam, Girish Sastry, Amanda Askell, Sandhini Agarwal, Ariel Herbert-Voss, Gretchen Krueger, T. J. Henighan, Rewon Child, Aditya Ramesh, Daniel M. Ziegler, Jeff Wu, Clemens Winter, Christopher Hesse, Mark Chen, Eric Sigler, Mateusz Litwin, Scott Gray, Benjamin Chess, Jack Clark, Christopher Berner, Sam McCandlish, Alec Radford, Ilya Sutskever, and Dario Amodei. 2020. [Language models are few-shot learners](#). *ArXiv*, abs/2005.14165.
- Xingyu Cai, Jiaji Huang, Yu-Lan Bian, and Kenneth Ward Church. 2021. [Isotropy in the contextual embedding space: Clusters and manifolds](#). In *International Conference on Learning Representations*.
- Pierre Carbonnelle. 2024. [Pypl popularity of programming language index](#).
- Tim Dettmers, Artidoro Pagnoni, Ari Holtzman, and Luke Zettlemoyer. 2023. [Qlora: Efficient finetuning of quantized llms](#). *ArXiv*, abs/2305.14314.
- William B. Dolan and Chris Brockett. 2005. [Automatically constructing a corpus of sentential paraphrases](#). In *International Joint Conference on Natural Language Processing*.
- Jian Gu, Aldeida Aleti, Chunyang Chen, and Hongyu Zhang. 2024. [Realizing disentanglement in lm latent space via vocabulary-defined semantics](#).

- Zeyu Han, Chao Gao, Jinyang Liu, Jeff Zhang, and Sai Qian Zhang. 2024. [Parameter-efficient fine-tuning for large models: A comprehensive survey](#). *ArXiv*, abs/2403.14608.
- Geoffrey E. Hinton. 2009. [Deep belief networks](#). *Scholarpedia*, 4:5947.
- Geoffrey E. Hinton. 2017. [Boltzmann machines](#). In *Encyclopedia of Machine Learning and Data Mining*.
- Geoffrey E. Hinton, Simon Osindero, and Yee Whye Teh. 2006. [A fast learning algorithm for deep belief nets](#). *Neural Computation*, 18:1527–1554.
- J. Edward Hu, Yelong Shen, Phillip Wallis, Zeyuan Allen-Zhu, Yuanzhi Li, Shean Wang, and Weizhu Chen. 2021. [Lora: Low-rank adaptation of large language models](#). *ArXiv*, abs/2106.09685.
- Radford M. Neal. 1992. [Connectionist learning of belief networks](#). *Artif. Intell.*, 56:71–113.
- Long Ouyang, Jeff Wu, Xu Jiang, Diogo Almeida, Carroll L. Wainwright, Pamela Mishkin, Chong Zhang, Sandhini Agarwal, Katarina Slama, Alex Ray, John Schulman, Jacob Hilton, Fraser Kelton, Luke E. Miller, Maddie Simens, Amanda Askell, Peter Welinder, Paul Francis Christiano, Jan Leike, and Ryan J. Lowe. 2022. [Training language models to follow instructions with human feedback](#). *ArXiv*, abs/2203.02155.
- Rui Pan, Xiang Liu, Shizhe Diao, Renjie Pi, Jipeng Zhang, Chi Han, and Tong Zhang. 2024. [Lisa: Layer-wise importance sampling for memory-efficient large language model fine-tuning](#). *ArXiv*, abs/2403.17919.
- Adam Paszke, Sam Gross, Francisco Massa, Adam Lerer, James Bradbury, Gregory Chanan, Trevor Killeen, Zeming Lin, Natalia Gimelshein, Luca Antiga, Alban Desmaison, Andreas Köpf, Edward Yang, Zach DeVito, Martin Raison, Alykhan Tejani, Sasank Chilamkurthy, Benoit Steiner, Lu Fang, Junjie Bai, and Soumith Chintala. 2019. [Pytorch: An imperative style, high-performance deep learning library](#). In *Neural Information Processing Systems*.
- Xuan Hieu Phan, Minh Le Nguyen, and Susumu Horiguchi. 2008. [Learning to classify short and sparse text & web with hidden topics from large-scale data collections](#). In *The Web Conference*.
- Colin Raffel, Noam M. Shazeer, Adam Roberts, Katherine Lee, Sharan Narang, Michael Matena, Yanqi Zhou, Wei Li, and Peter J. Liu. 2019. [Exploring the limits of transfer learning with a unified text-to-text transformer](#). *J. Mach. Learn. Res.*, 21:140:1–140:67.
- Babak Rokh, Ali Azarpeyvand, and Alireza Khantey-moori. 2022. [A comprehensive survey on model quantization for deep neural networks in image classification](#). *ACM Transactions on Intelligent Systems and Technology*, 14:1 – 50.
- Baptiste Rozière, Jonas Gehring, Fabian Gloeckle, Sten Sootla, Itai Gat, Xiaoqing Tan, Yossi Adi, Jingyu Liu, Tal Remez, Jérémy Rapin, Artyom Kozhevnikov, I. Evtimov, Joanna Bitton, Manish P Bhatt, Cristian Cantón Ferrer, Aaron Grattafiori, Wenhan Xiong, Alexandre D’efosse, Jade Copet, Faisal Azhar, Hugo Touvron, Louis Martin, Nicolas Usunier, Thomas Scialom, and Gabriel Synnaeve. 2023. [Code llama: Open foundation models for code](#). *ArXiv*, abs/2308.12950.
- Elvis Saravia, Hsien-Chi Toby Liu, Yen-Hao Huang, Junlin Wu, and Yi-Shin Chen. 2018. [Carer: Contextualized affect representations for emotion recognition](#). In *Conference on Empirical Methods in Natural Language Processing*.
- David R. So, Chen Liang, and Quoc V. Le. 2019. [The evolved transformer](#). In *International Conference on Machine Learning*.
- Richard Socher, Alex Perelygin, Jean Wu, Jason Chuang, Christopher D. Manning, A. Ng, and Christopher Potts. 2013. [Recursive deep models for semantic compositionality over a sentiment treebank](#). In *Conference on Empirical Methods in Natural Language Processing*.
- TIOBE. 2024. [Tiobe index | tiobe - the software quality company](#).
- Hugo Touvron, Thibaut Lavril, Gautier Izacard, Xavier Martinet, Marie-Anne Lachaux, Timothée Lacroix, Baptiste Rozière, Naman Goyal, Eric Hambro, Faisal Azhar, Aurelien Rodriguez, Armand Joulin, Edouard Grave, and Guillaume Lample. 2023. [Llama: Open and efficient foundation language models](#). *ArXiv*, abs/2302.13971.
- Ashish Vaswani, Noam M. Shazeer, Niki Parmar, Jakob Uszkoreit, Llion Jones, Aidan N. Gomez, Lukasz Kaiser, and Illia Polosukhin. 2017. [Attention is all you need](#). *ArXiv*, abs/1706.03762.
- Roman Vershynin. 2018. *Random Vectors in High Dimensions*, page 38–69. Cambridge Series in Statistical and Probabilistic Mathematics. Cambridge University Press.
- Ellen M. Voorhees and Dawn M. Tice. 2000. [Building a question answering test collection](#). In *Annual International ACM SIGIR Conference on Research and Development in Information Retrieval*.
- Jason Wei, Yi Tay, Rishi Bommasani, Colin Raffel, Barret Zoph, Sebastian Borgeaud, Dani Yogatama, Maarten Bosma, Denny Zhou, Donald Metzler, Ed Chi, Tatsunori Hashimoto, Oriol Vinyals, Percy Liang, Jeff Dean, and William Fedus. 2022. [Emergent abilities of large language models](#). *ArXiv*, abs/2206.07682.
- Thomas Wolf, Lysandre Debut, Victor Sanh, Julien Chaumond, Clement Delangue, Anthony Moi, Pierric Cistac, Tim Rault, Rémi Louf, Morgan Funtowicz,

and Jamie Brew. 2019. Transformers: State-of-the-art natural language processing. In *Conference on Empirical Methods in Natural Language Processing*.

Xiaoxia Wu, Cheng Li, Reza Yazdani Aminabadi, Zhewei Yao, and Yuxiong He. 2023. [Understanding int4 quantization for language models: Latency speedup, composability, and failure cases](#). In *International Conference on Machine Learning*.

Ligeng Zhu, Lanxiang Hu, Ji Lin, and Song Han. 2024. [LIFT: Efficient layer-wise fine-tuning for large model models](#).

## A Implementation Details

### A.1 Environments

Our implementation uses deep learning framework PYTORCH (Paszke et al., 2019), TRANSFORMERS (Wolf et al., 2019), and use PEFT<sup>2</sup> to conduct the LoRA experiments. The LM finetuning experiments are based on existing PEFT methods, specifically LORA (Hu et al., 2021). We use quantization techniques (INT4) to load Llama3-8B, with the default settings (Dettmers et al., 2023; Wu et al., 2023), which reduces the memory cost in LM finetuning with slight performance loss.

The experiments are conducted via a single run, with the global random-seed 42. The computation is based on a single Nvidia A100 (80 GB), and the computation budget is around 500 GPU hours.

### A.2 License and Terms

We understand and respect the licenses used in our experiments, including the Apache-2.0 license for Pythia models<sup>3</sup> and the Llama3 community license<sup>4</sup>. We confirm that our use of existing artifacts was consistent with their intended use.

### A.3 SEFT Algorithm with Budget

By introducing the budget for LM finetuning, our semantic-based layer-freezing approach can fulfill the intended computation cost. Then, to guarantee improved performance, we propose the SEFT algorithm with the budget consideration, as shown in Algorithm 4. The intent of the code is intuitive: first, compute the deviations to find the eof-layer for each data; then, arrange the data with the similar eof-layers into the budget; last, gradually narrow down the scope of finetuning (freezing more model layers), and use the arranged data to backpropagate the loss. In the pseudocode, at the 15-th line

of code, the invoked SEFT function is mentioned as Algorithm 3. For the sake of the sequential access restriction of data-loader, the algorithm is described with the for-loops and the repeated iterations. In the implementation, we can choose to use random access and caching techniques to remove the for-loops and reduce the number of iterations.

---

#### Algorithm 4 SEFT Layer-Freezing w/ Budgets

---

**Require:** optimizer, data\_loader, budgets

**Ensure:** NONE

```

1: tabu_ids ← empty list
2: for layer_id ← 0 to layer_num do
3:   # (a) freeze layers from deep to shallow
4:   freeze_layers(range(0, layer_id))
5:   # Backpropagation of Matching Data
6:   for batch_id, batch in data_loader do
7:     # (b) check whether to jump the loop
8:     if budgets[layer_id] == 0 then
9:       break
10:    end if
11:    if batch_id in tabu_ids then
12:      continue
13:    end if
14:    # (c) check whether to backpropagate
15:    eof_layer_id ← SEFT(
16:      get_latent_reprs(batch),
17:      get_semantic_anchors(batch))
18:    if eof_layer_id > layer_id then
19:      continue
20:    end if
21:    # (d) backpropagate and update states
22:    optimizer.zero_grad()
23:    loss ← compute_loss(batch)
24:    loss.backward()
25:    optimizer.step()
26:    budgets[layer_id] -= 1
27:    tabu_ids.append(batch_id)
28:  end for
29:  # Backpropagation of Remaining Data
30:  for batch_id, batch in data_loader do
31:    # (b) check whether to jump the loop
32:    ... # repeat the code block
33:    # (d) backpropagate and update states
34:    ... # repeat the code block
35:  end for

```

---

<sup>2</sup><https://github.com/huggingface/peft>

<sup>3</sup><https://github.com/EleutherAI/pythia>

<sup>4</sup><https://llama.meta.com/llama3/license/>

Variant	Dataset					Avg.
	CARER	MRPC	SST5	TREC	WebSS	
LIFT[ <code>half</code> ][ <code>sam</code> ]	0.827	0.771	0.590	0.948	0.898	0.807
LIFT[ <code>half</code> ][ <code>fc</code> ]	0.348	0.665	0.286	0.954	0.132	0.477
LIFT[ <code>half</code> ][ <code>both</code> ]	0.348	0.665	0.286	0.130	0.132	0.312
SEFT[ <code>half</code> ][ <code>sam</code> ]	0.923	0.737	0.579	0.964	0.904	0.821
SEFT[ <code>half</code> ][ <code>fc</code> ]	0.348	0.665	0.286	0.978	0.646	0.584
SEFT[ <code>half</code> ][ <code>both</code> ]	0.348	0.665	0.286	0.974	0.909	0.636

Table 7: Accuracy of layer-freezing methods when finetuning different modules (on the diverse datasets, using Llama3-8B).

## B More Analysis

### B.1 LM Finetuning on Modules

We study which modules in LM layers are more worthy for model finetuning, to avoid the bias by LORA, since the vanilla implementation of LORA is centered on the self-attention module (`sam`). We adapt LORA to make it capable of finetuning the fully-connected module (`fc`). We denote the variants with different modules for finetuning with `[half][sam]`, `[half][fc]`, and `[half][both]`, representing the cases where only self-attention modules, or only fully-connected modules, or both two types of modules are finetuned.

As shown in Table 7, for both LIFT and SEFT, finetuning `[half][sam]` is more beneficial than finetuning `[half][fc]` and `[half][both]`. Besides, SEFT variants are better than the corresponding LIFT variants when the finetuning is on different modules. It means, for LM finetuning, the effects on self-attention modules are more obvious than on fully-connected modules. From the perspective of semantic transition, the conclusion still stands. And also, our approach SEFT performs better than the baseline when finetuning different modules.

By focusing on the self-attention modules, LM finetuning can realize efficient and impactful finetuning (Hu et al., 2021). It is due to the critical role of self-attention module in capturing the relations between the tokens in the given inputs (Vaswani et al., 2017). In intuitive thinking, the effect of finetuning both modules shall be better, since more parameters are trainable. However, `[half][both]` did not obtain better performance. Again, this finding supports our claim on efficient fine-tuning that, *if it is known in advance which parameters are worth being trainable, LM fine-tuning may yield better results at less computation cost.*

### B.2 Effects of LM Finetuning

To study the effects of our SEFT approach to LM finetuning, we illustrate the deviation changes in

LM finetuning of two settings: one is making all layers trainable, corresponding to `Navie[full]`, as shown in Figure 4; while the other one is taking our approach for layer freezing, corresponding to `SEFT[half]`, as shown in Figure 5.

In the illustrations, the deviations are in the range of  $[0, 2]$ , since it is derived from the cosine similarity. Besides, in a high-dimensional latent space, the representations tend to be orthogonal to others (including the semantic anchors) (Vershynin, 2018), so when the deviations are smaller than 1, it means the corresponding data representations are steering towards the ground truth, then the corresponding LM predictions may be correct. Otherwise, if the deviations are larger than 1, then the corresponding LM predictions are not likely to be correct.

By comparing the illustrated two situations of the blue shapes, we conclude the advantages of our semantic-based layer-freezing approach to LM finetuning as: our approach can avoid the side effects of LM finetuning to deep layers, and tends to make the transition deviations in shallow layers small. Taking the illustrated situation of the red shapes as a reference, we believe that the first advantage (on the side effects to the deep layers) may be the cause of the second advantage (on the small deviations in shallow layers). It explains why our approach lead to small deviations in shallow layers, and also, it emphasizes the importance of reducing the deviations in deep layers. Further, the causation explains how to achieve better performance while reducing the computation cost in LM finetuning.

In addition, based on the illustrations, we see the accumulated effects of our approach in reducing the deviations in the last few model layers, where the blue shapes gradually move to lower positions, which indicates lower deviations of the data and the higher likelihood of correct LM predictions.

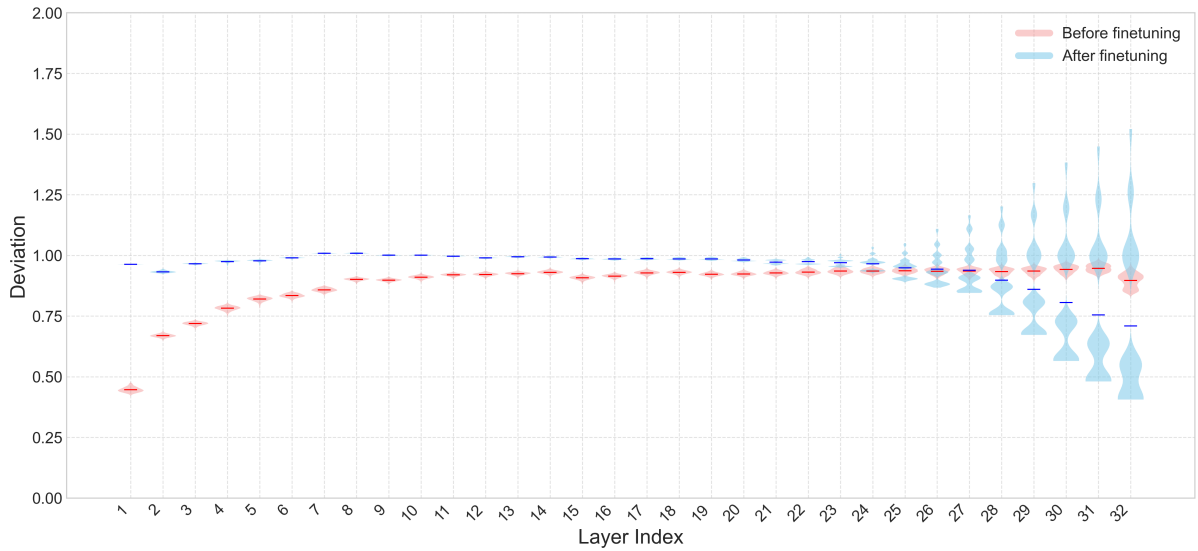


Figure 4: Violin plot of the deviations of each layer in LM finetuning, where the crossbars represent the mean of deviations, when making all model layers trainable (on the CARER dataset, using Llama3-8B). The phenomena include: (1) The red crossbars usually lie at lower positions than the blue crossbars (in the first 27 layers). It means, the deviation changes by LM finetuning are negative in most layers. (2) The blue shapes are flattened in the last few layers (from the 25-th layer to the last-layer) but some areas in the shapes lie at higher positions. It means, the distribution of the deviations in the last layers is forming multiple peaks, no longer centered in only one peak, and lots of data show higher deviations; (3) The differences between red and blue are large and show a reversal (first red is better, then blue is better) in the first and last few layers. It means, the deviation changes by LM finetuning are significant, which are worse in the deeper layers but better in the shallower layers.

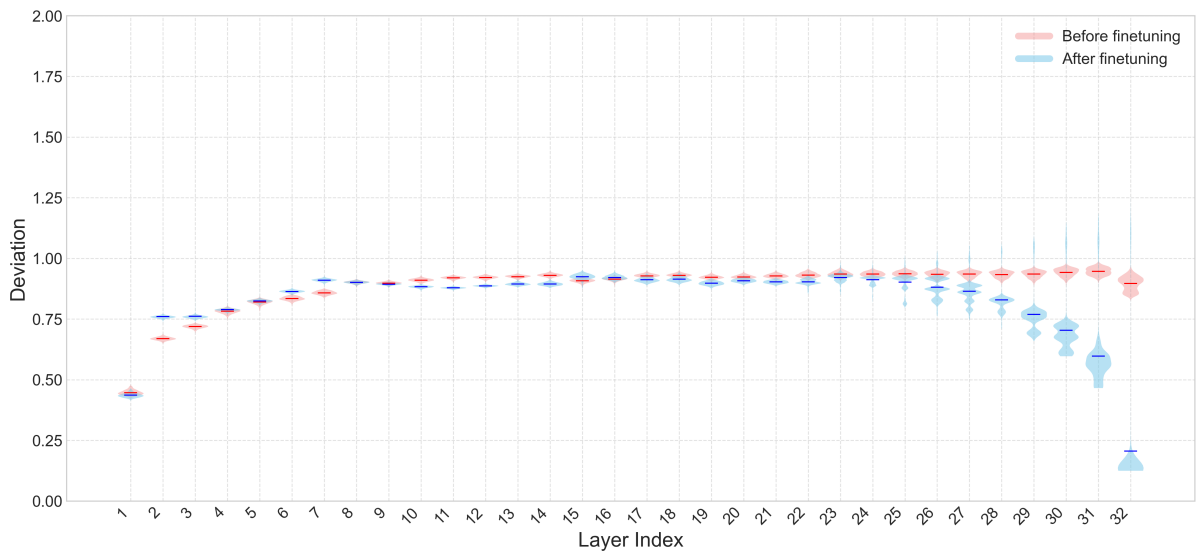


Figure 5: Violin plot of the deviations of each layer in LM finetuning, where the crossbars represent the mean of deviations, when taking semantic-based layer-freezing (on the CARER dataset, using Llama3-8B). The phenomena include: (1) The red crossbars usually lie at the same positions as the blue crossbars (in the first 27 layers). It means, the deviation changes by LM finetuning are very small in most layers. (2) The blue shapes are flattened in the last few layers (from the 25-th layer to the last-layer) but almost all areas in the shapes lie at lower positions. It means, the distribution of the deviations in the last layers is forming multiple peaks, no longer centered in only one peak, and almost all data show lower deviations; (3) The differences between red and blue are only getting large (blue is better) in the last few layers. It means, the deviation changes by LM finetuning are positive and highly targeted, which are mainly in the shallower layers.